

# Design of SMPS Buck Converter with Protection Circuits for Automotive Charger

Raveena Jokim Crastha, Roopa M

**Abstract:** The automotive manufacturers are working towards enhancing sophisticated designs and technologies that enable better vehicle-user connectivity by integrating all the control units to one infotainment system. This key feature with high-level intelligence and competency plays an important role with an increase in demand in the production process of the automotive industry. This paper proposes a unique design of USB smart charger module that is designed in a way to fit into limited space in a front panel of the vehicle. The specific design methodology of the DC-DC SMPS buck converter with the protection circuits which serves as the important section of the smart charger is explained. The module is designed with both single and double port that are identical to each other. Each of these models provides effective connectivity of devices in the vehicle network with secured over-current, over-voltage and short circuit protection circuitry. The configuration of controllers and connectors used is implemented in Altium. The functionality of the system designed is examined and verified in TINA-TI tool.

**Keywords:** Electromagnetic Compatibility, Switched Mode Power Supply, Universal Serial Bus.

## I. INTRODUCTION

The OEMs in the automotive sector are targeting towards the development in differentiating the vehicle designs with compact and more functionality which is of greater competitive advantage. With this approach the USB smart Charger module is designed that supports in acquiring automotive grade durability and achieves higher throughput while occupying less space in the front panel of the vehicle. The smart charger module is designed with both single and dual ports that are identical and comes with the protection circuits that serve specific operations with safety concern. This paper approaches the specified construction of the DC-DC SMPS buck converter with the protection circuits which serves as the important section of the smart charger. As the battery capacity and the charging rate increases more space is required dispose the heat generated and to improve the efficiency thus, the method implemented allows to reduce the board size and to remove the heat from the load [1][2][3].

In this paper the module is designed for a power input of 9V-16V. The input battery supply may consist of variant pulses due to different load conditions or charge management. These sudden high transient voltages could damage the components along the line of operation significantly. Thus, the power input is followed by the bidirectional clamping surge protection circuit to control the load dump. The system is operated with the switching frequency of 400Khz. The increase in switching frequency invites certain limitations such as the performance of the necessary parts gets restricted, and the efficiency of the system gets affected by the parasitic losses [6][5]. Hence, the effective high-capacity EMC  $\pi$  filter is designed to control these magnetic effects. The undervoltage and overvoltage are adjusted along with the proper frequency synchronization and inrush control that develops the power handling capability of the overall system with automotive durability. The SMPS buck converter is constructed to provide regulated output of 5V and the higher current rating along with an under-voltage protection and the inrush current control that contributes to achieve higher efficiency. The converter is followed by the current limiting switch that controls the overcurrent protection limit with guaranteed output of 2.4A and 3A to Type A and Type C USB downstream ports respectively. The modules are designed in both single and double ports that are identical and provides effective and reliable connectivity of device in the vehicle network.

## II. DESIGN REQUIREMENTS

The block diagram of the proposed design is shown in Fig.1. The USB smart charger module employs the input battery voltage of 9V-16V with the operating temperature range -40°C to 125°C that supports in achieving automotive grade durability. The regulated output voltage is step down to 5V using SMPS Buck converter that is required for application with an output power of 30W and output current of 6A.

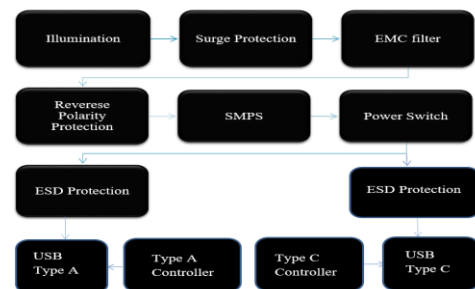


Fig. 1. Block diagram of SMPS Buck Converter with Protection Circuits – Automotive Charger

Manuscript received on June 19, 2021.

Revised Manuscript received on June 26, 2021.

Manuscript published on June 30, 2021.

\* Correspondence Author

Ms. Raveena Jokim Crastha\*, Master's, Digital Electronics and Communication Specialization, Dayananda Sagar College of Engineering, Bengaluru, India.

Dr. Roopa M, Professor, Department of Electronics and Communication at Dayananda Sagar College of Engineering, Bengaluru, India.

© The Authors. Published by Blue Eyes Intelligence Engineering and Sciences Publication (BEIESP). This is an open access article under the CC BY-NC-ND license (<http://creativecommons.org/licenses/by-nc-nd/4.0/>)

The dynamic performance is estimated by considering switching frequency of 400kHz with an input and output voltage ripple of 100mV and 50mV respectively. The output current from the buck is controlled by the current limit switch to provide an input current of 2.4A and 3A to the Type A and Type C USB ports that support in charging and data transfer. The design requirements are shown in Fig.2

| Parameters                       | Values         |
|----------------------------------|----------------|
| Input Voltage, V <sub>IN</sub>   | 9V – 16V       |
| Nominal V <sub>IN</sub>          | 12V            |
| Output Voltage, V <sub>OUT</sub> | 5V             |
| Output Current                   | 6A             |
| Switching Frequency              | 400kHz         |
| Power                            | 30 Watts       |
| Temperature                      | -40°C to 125°C |
| Input Voltage ripple             | 100mV          |
| Output Voltage ripple            | 50mV           |

**Fig. 2.Design requirements for the system**

## III. DESIGN METHODOLOGY

In this section the proposed design implementation of the automotive charger is structured as per the requirements. The first sub-section explains about automotive transient's protection, followed by designing EMC  $\pi$  filter for the appropriate switching frequency considered, reverse polarity protection, SMPS buck converter design and USB Type A and Type C controller and connector implementations are explained in further sub-sections.

### A. Automotive Surge Protection

The surge protector is used to protect the device from the sudden voltage transients that can damage the devices in the circuit. The principle of the surge protection is to limit the voltage across the devices by either grounding or blocking the transients above the threshold [15]. The module is designed according to the EMC standards for automotive compliance [16] against pulses ISO 7376-2 that are caused due to electrical disturbance from coupling and conduction. This includes Pulse 1- due to disconnection of the supply from the inductive load, Pulse 2a – due to inductive kick of wiring harness, Pulse 3a and 3b – due to switching process and Pulse 5b – due to load dump and ISO 16750-2 for environmental conditions and testing for electrical and electronic equipment as shown in Fig.3. The Surge protector device is connected parallel to the circuit as shown in the Fig.4. Under normal operation the diode acts as an open circuit by presenting high impedance path to the protected circuit model. When the voltage exceeds the threshold, the TVS diode acts as a closed circuit with a low impedance path by diverting the transient current to the ground and limits the voltage across the protected circuit by clamping it to the TVS diode voltage

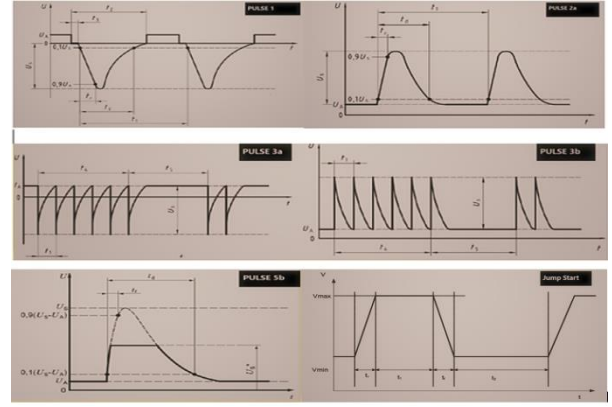


**Fig. 3.EMC standard ISO 7376-2 and ISO 16750-2 pulses**

### B. Design of EMC II Filter

The EMC (Electro-magnetic Compatibility) control includes the suppression of the noise generation and the self-prevention of incoming noise quantities. The demand for the higher performance of the applications with increase in frequency results in electromagnetic interferences [11][12]. The differential mode noises generated, flows along the signal power and current but with different inward and outward directions that can be suppressed with the help of  $\pi$  filter [13] in which the inductors are connected in series and the capacitors are connected in parallel between the conducting lines. This helps in filtering the noise coming from the input of the DC-DC converter.

| Service /Band | Frequency MHz | Levels (dBμV) |    |         |    |         |    |         |    |         |    |
|---------------|---------------|---------------|----|---------|----|---------|----|---------|----|---------|----|
|               |               | Class 1       |    | Class 2 |    | Class 3 |    | Class 4 |    | Class 5 |    |
|               |               | PK            | GP | PK      | GP | PK      | GP | PK      | GP | PK      | GP |
| LW            | 0.15-0.3      | 110           | 97 | 100     | 87 | 90      | 77 | 80      | 67 | 70      | 57 |
| MW            | 0.53-1.8      | 86            | 73 | 78      | 65 | 70      | 57 | 62      | 49 | 54      | 41 |
| SW            | 5.9-6.2       | 77            | 64 | 71      | 58 | 65      | 52 | 59      | 46 | 53      | 40 |
| FM            | 76-108        | 62            | 49 | 56      | 43 | 50      | 37 | 44      | 31 | 38      | 25 |
| TV Band I     | 41-88         | 58            | -  | 52      | -  | 46      | -  | 40      | -  | 34      | -  |
| CB            | 26-28         | 68            | 55 | 62      | 49 | 56      | 43 | 50      | 37 | 44      | 31 |
| VHF           | 30-54         | 68            | 55 | 62      | 49 | 56      | 43 | 50      | 37 | 44      | 31 |
| VHF           | 68-87         | 62            | 49 | 56      | 43 | 50      | 37 | 44      | 31 | 38      | 25 |

| Service /Band | Frequency MHz | Levels (dBμV) |         |         |         |         |
|---------------|---------------|---------------|---------|---------|---------|---------|
|               |               | Class 1       | Class 2 | Class 3 | Class 4 | Class 5 |
|               |               | AVG           | AVG     | AVG     | AVG     | AVG     |
| LW            | 0.15-0.3      | 90            | 80      | 70      | 60      | 50      |
| MW            | 0.53-1.8      | 66            | 58      | 50      | 42      | 34      |
| SW            | 5.9-6.2       | 57            | 51      | 45      | 39      | 33      |
| FM            | 76-108        | 42            | 36      | 30      | 24      | 18      |
| TV Band I     | 41-88         | 48            | 42      | 36      | 30      | 24      |
| CB            | 26-28         | 48            | 42      | 36      | 30      | 24      |
| VHF           | 30-54         | 48            | 42      | 36      | 30      | 24      |
| VHF           | 68-87         | 42            | 36      | 30      | 24      | 18      |

**Fig. 4.CISPR 25 limits**

### Fig. 5.

Let us consider the estimated efficiency to be 96%, thus the duty cycle as per the requirement will be,

$$\text{Duty Cycle (D)} = \frac{V_{(out)} \times \eta}{V_{(min)}} = 0.533 \quad (1)$$

Corner Frequency,  $f_c$

$$f_c = \frac{f_s}{10} = \frac{400kHz}{10} = 40kHz \quad (2)$$

The differential mode filtering inductor,  $L_d$  can be within range 1μH - 10μH with maximum current carrying capacity. The inductor of value 4.7 μH is selected. The switching frequency of 400khz is considered. The filtering capacitor,  $C_f$  can be estimated as following.

$$C_{(fa)} = \frac{C_{(in)}}{C_{(in)}L_d\left(\frac{2\pi f_s}{10}\right)^2} - 1 = 3.7\mu F$$

(3)

$$C_{(fb)} = \frac{1}{L_d} \left( \frac{10}{2\pi f_s} \right)^2 = 0.45\mu F$$

(4)

where,

$$|ATT|_{dB} = 20 \log \left( \frac{\frac{1}{\pi^2 f_s C_{(in)}} \sin(\pi D)}{1\mu V} \right) - V_{max} = 22.54dB$$

(5)

The maximum value between (3) and (4) should be considered as filtering capacitor. Therefore,  $C_f = C_{(fb)} = 3.7\mu F$

where,

$f_s$  = Switching Frequency

$C_{(in)}$  = Input Capacitor

$L_d$  = Differential mode Inductor

$|ATT|_{dB}$  = Attenuation of the filter design and based of requirements

$V_{max}$  = maximum noise level disturbances as per CISPR 25 class- 5

The electrolytic damping capacitor and the ESR should be,

$$C_d > 150 \mu F$$

$$ESR = \sqrt{\frac{L_d}{C_{in}}} = 0.35 \Omega$$

(6)

The ripple current is to be 30% of maximum output current. The 4.32mV conducted emissions of the module for 400kHz of switching frequency is estimated to be 72.7dBV. According to CISPR 25 class 5, the specifications for conducted emissions are not specified for 400kHz instead, they are specified for 530kHz (i.e., 54dBμV). Hence the module needs to attenuate at least of 18.7dB. The construction of  $\pi$  filter module is depicted in Fig.5.

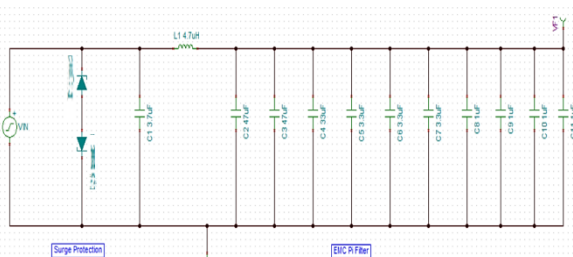


Fig. 6. Construction of Surge Protection and EMC II Filter

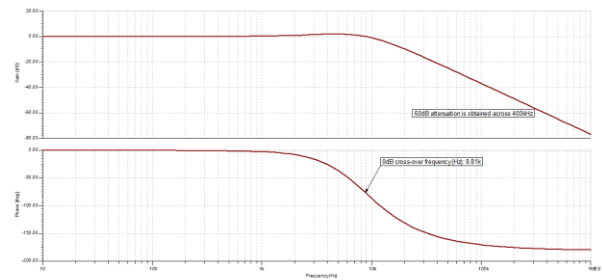


Fig. 7. Bode plot - EMC II Filter  
Fig. 8.

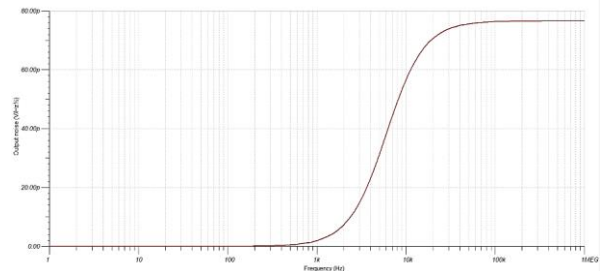


Fig. 9. Output noise Vs Frequency plot

### C. Reverse Polarity Protection

The switching regulators are not protected against reverse polarity which might cause a failure in the system operation [9]. Hence the converters must be protected from the swapping of the input terminals / change in polarity [7] [14]. This is implemented as shown in Fig.8 using Automotive grade qualified hide side protection controller. It controls the inrush current, supports programmable Under-voltage lockout conditions and adjustable overvoltage protection with automatic restart after the shutdown condition. The different operational of the protection circuit is shown in Fig.9, Fig.10 and Fig.11.

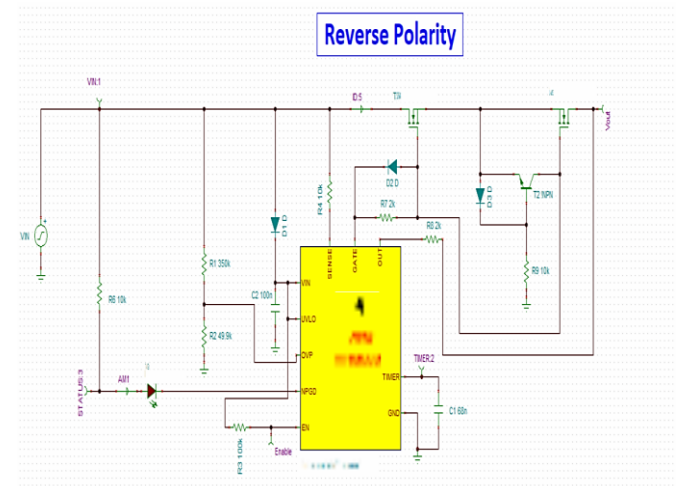


Fig. 10. Construction of Reverse Polarity Protection

Case 1. When positive voltage of 12V is applied

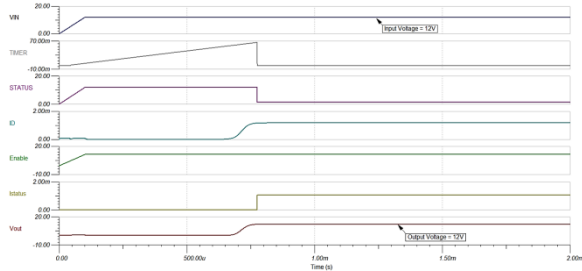


Fig. 11. Simulated output - Case I

Case 2. When negative voltage of -12V is applied

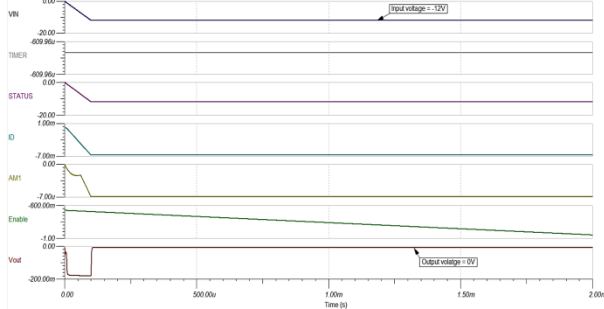


Fig. 12. Simulated output - Case II

Case 3. When over voltage of 17V is applied

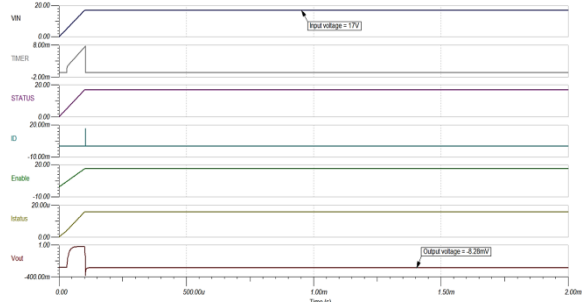


Fig. 13. Simulated output - Case III

#### D. Design of SMPS Buck Converter

The switching regulators are used to generate high power efficiency conversion to control a well-regulated supply voltage to the systems [8]. The switching regulators are designed with the help of the transistors that acts as a switch by being completely turned ON or OFF. The synchronous buck converter rectification scheme is designed to reduce the voltage drop and to attain the better performance of the circuit by using MOSFET that has very low  $R_{ds-ON}$  resistance and the implementation of the same is shown in Fig.12.

Undervoltage lockout (UVLO) pin is designed using voltage divider resistors  $R_{UV1}$  and  $R_{UV2}$  to disable the functions below the input start-up voltage,  $R_{UV1}$  and  $R_{UV2}$  are considered to be  $16k\Omega$  and  $100k\Omega$  respectively.

The inductor value is determined by setting the output ripple current to be 30% of output current whose value is 6A, output voltage and maximum input voltage.

$$L_o = \frac{V_{out}}{I_{pp(max)} \times f_{sw}} \times \left(1 - \frac{V_{out}}{V_{in(max)}}\right) = 4.7\mu H \quad (7)$$

To emulate the positive slope of the inductor. The  $C_{Ramp}$  is set to 820pF.  $R_{Ramp}$  is calculate as shown. The current amplification gain,  $A_s$  is taken as 10.

$$R_{Ramp} = \frac{L_o}{K \times C_{Ramp} \times R_s \times A_s} \quad (8)$$

Feedback resistors,  $R_{fb1}$  and  $R_{fb2}$  are designed to set the output voltage level.

$$\frac{R_{fb2}}{R_{fb1}} = \frac{V_{out}}{0.8V} - 1 \quad (9)$$

The compensation pin is connected to  $R_{Comp}$ ,  $C_{Comp}$  and  $C_{Hf}$  to achieve stable output voltage gain and to maintain the phase characteristics.

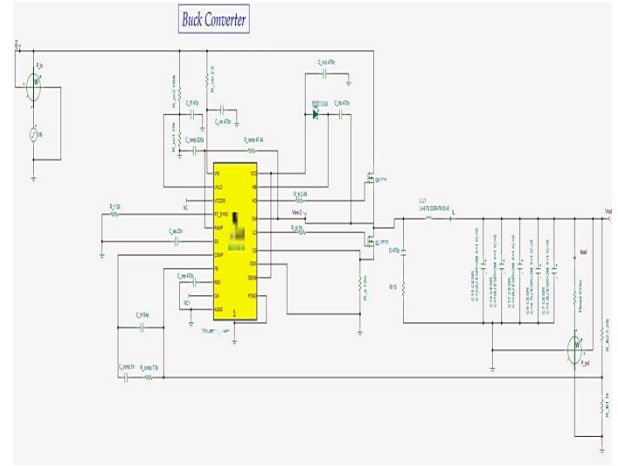


Fig. 14. Construction Of Smps Buck Converter

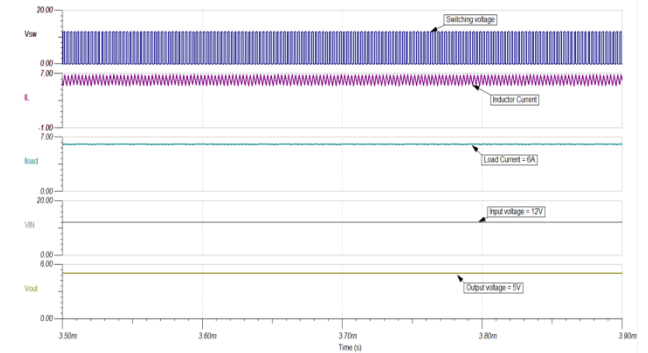


Fig. 15. Simulated output - SMPS Buck Converter

#### E. USB Type-A and Type-C Controllers and Connectors

The USB plug and play peripheral interface maintains a universal standard to manage the power requirements that ensures host, and the client devices are operated together. The USB has a power capability to charge the batteries of the portable devices attached that optimizes the user experience. These portable devices need a method to determine the amount of power to be drawn by the USB ports to support charging and its normal operation [4][10]. The scheme was introduced in the USB Battery Charging Specification Revision 1.2, released in the year 2010. It is also called as BC 1.2, established as the critical standard to charge the battery from a port.



The standard BC 1.2 mechanisms is expected to operate in the presence of D+ and D- data lines within the USB cable. Otherwise, the devices are limited to draw maximum current of 100mA. The Proposed module is designed for a DCP charging profile port and the USB Type A and Type C are chosen according to the BC 1.2 Standard. The output current from the buck is controlled by the current limit switch to provide an input current of 2.4A and 3A to the Type A and Type C USB ports that supports charging.

### 1) USB Type A Controller and Connector Implementation

The Type A USB controller supports the automatic detection of DCP profile and selects D+ and D- lines settings accordingly to support fast charging. It is integrated with the programmable current limits across the port when the adjacent ports are experiencing heavy loads. Current Limit Settings, ILIM\_HI and ILIM\_LO are configured through external independent resistors namely  $R_{(ILIM\_HI)}$  and  $R_{(ILIM\_LO)}$  to approximate the maximum and minimum values of the current to milliamperes for design purposes. A single port I/O receptable shielded Type A connector is used. The implementation of the same is shown in Fig.14 and Fig.15

$$I_{(OS\_min)}(mA) = \frac{50409(V)}{R_{(ILIM\_LO)}^{0.9982}(k\Omega)} - 35 = 2150$$

(10)

$$I_{(OS\_max)}(mA) = \frac{57813(V)}{R_{(ILIM\_HI)}^{1.01072}(k\Omega)} + 41 = 2973$$

(11)

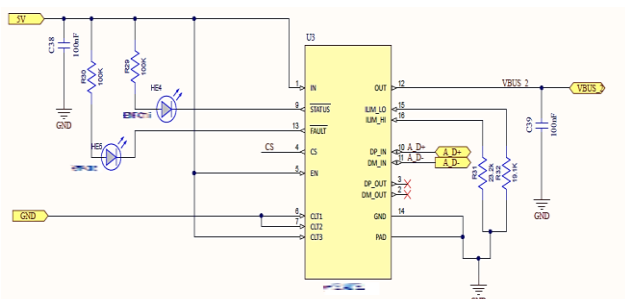


Fig. 16. Construction of USB Type – A Controller in ALTIUM

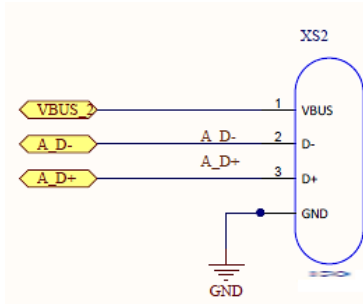


Fig. 17. Construction of USB Type – A Connector in ALTIUM

### 2) USB Type C Controller and Connector Implementation

The Type C is a downstream facing port controller monitors the configuration channel lines to detect the connected devices through power switch. The current

capability  $V_{BUS}$  is communicated with the upstream facing ports through configuration channel lines and identifies the audio accessories attached to it. The power management resources are optimized across multi ports. It has wide range of applications over automotive charging and infotainment systems. The device supports BC 1.2 critical charging standard through the connections made across D+ and D- data lines. The low capacitance ESD protection array is connected to the controller to protect sensitive components connected across the interface lines. The device holds the pair of diodes across each channel thus, protecting the internal circuitry from  $\pm 15kV$  ESD pulses by providing the safe discharge path to dissipate the energy associated with the ESD strikes. This results in the proper functionality of the core circuitry of the system board designed. The single port I/O receptable shielded type connector is used and the implementation of the same is shown in Fig.16 and Fig.17.

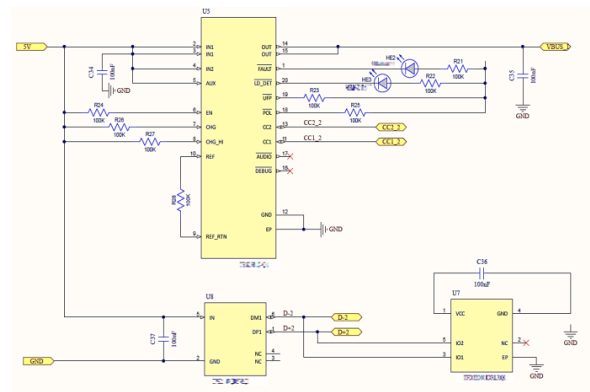


Fig. 18. Construction of USB Type – C Controller in ALTIUM

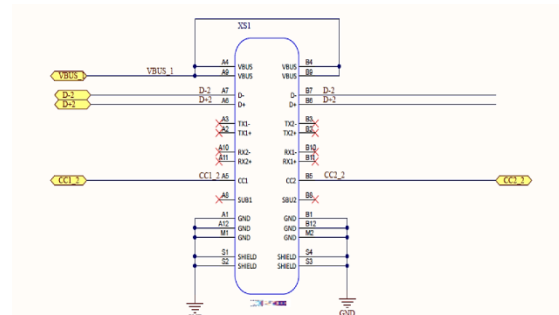


Fig. 19. Construction of USB Type – C Connector in ALTIUM

## IV. RESULT AND DISCUSSION

- The surge protection configuration shown in the Fig.5 is designed to withstand the EMC standard automotive transients that are due to the electrical disturbances and environmental testing conditions. The wide range frequency range of voltage ripples gets generated due to the switching process in addition with the switching frequency taken into consideration for the design. This noise gets coupled further with the remaining protected circuits. Hence EMC  $\pi$  filter is designed to smooth down the voltage perturbations and to attain an attenuation of 18.7dB.

- The larger values of capacitors used, reduces the corner frequency, and increases the attenuation as shown in Fig.6. The attenuation is observed to be 60dB across 400kHz, switching frequency.
- The output noise is also observed to be in Pico range of voltages as shown in Fig.7.
- The switching regulators are not protected against reverse polarity which might cause a failure in the system operation. The reverse polarity protection circuit can be analyzed in three cases as shown in Fig.9, Fig.10 and Fig.11. Firstly, when the positive nominal voltage of 12V is applied across the protection circuit the output voltage will be without any distortion. In case 2, when a negative voltage is applied, the output is observed to be zero by protecting the module from the reverse polarity condition. The protector circuit is also designed for the overvoltage condition that is the output is expected to be zero when applied voltage is beyond the maximum power supply voltage required for the design.
- The synchronous buck converter allows frequency synchronization, undervoltage, thermal shutdown and slope compensation. The voltage below the minimum requirement is discarded as per the design. As shown in Fig.13 the output voltage is bucked down to 5V and the peak value of the inductor current is taken as 30% of output current of the regulator. The output current is observed to be 6A, which will be divided within the USB Type A and Type C controllers according to the design.
- The controllers are supported by the ESD protection. The configurations of USB Type A and Type C controllers and connectors are implemented in ALTIIUM.

## V. CONCLUSION

This paper approaches the USB smart Charger module design that supports in acquiring automotive grade durability and in achieving higher throughput while occupying less space in the front panel of the vehicle. The design consideration and the method of implementation of the DC-DC switch mode regulated power supply with protection circuits that serves specific operations with the safety concern was discussed. The components used in the design are all AEC-Q qualified and guarantees reliability. The Output was observed as per our design requirements that passes all the protection circuitry designed and leads to be 5V and 6A. The output current from the converter is limited to 2.4A and 3A to USB Type A and Type C respectively. The total efficiency is observed to be 95.6% as shown in Fig.18 This is almost equal to the estimated efficiency of 96%. The higher value of attenuation is achieved for the designed switching frequency. The functionality of the system is observed in TINA-TI simulator.

$$\eta = \frac{\text{Output Power}}{\text{Input power}} = \frac{29.99}{31.36} = 95.6\% \quad (12)$$

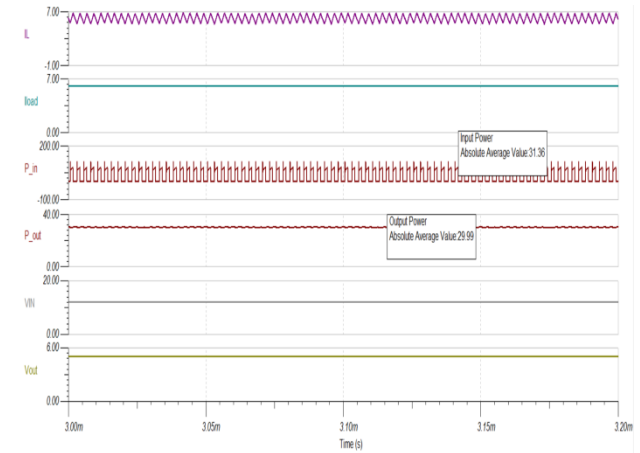


Fig. 20. System efficiency

## REFERENCES

1. R. Goel, G. Seo and H. Le, "A smart-USB-cable buck converter with indirect control," 2017 IEEE 18th Workshop on Control and Modeling for Power Electronics (COMPEL), Stanford, CA, 2017, pp. 1-6, doi: 10.1109/COMPEL.2017.8013370.
2. X. Ke, K. Wei and D. B. Ma, "A 10MHz, 40V-to-5V clock-synchronized AOT hysteretic converter with programmable soft start technique for automotive USB chargers," 2017 IEEE Applied Power Electronics Conference and Exposition (APEC), Tampa, FL, 2017, pp. 2146-2149, doi: 10.1109/APEC.2017.7930996.
3. K.L.Venkatesh and Sairam Chappidi "Portable USB Mobile Charger", short paper VIT University,Vellore, Tamil Nadu, India.Submitted 06 August 2015.
4. F. He, "USB Port and power delivery: An overview of USB port interoperability," 2015 IEEE Symposium on Product Compliance Engineering (ISPC), Chicago, IL, 2015, pp. 1-5, doi: 10.1109/ISPC.2015.7138710.
5. C. Hardy and H. Le, "8.3 A 10.9W 93.4%-Efficient (27W 97%-Efficient) Flying-Inductor Hybrid DC-DC Converter Suitable for 1-Cell (2-Cell) Battery Charging Applications," 2019 IEEE International Solid- State Circuits Conference - (ISSCC), San Francisco, CA, USA, 2019, pp. 150-152, doi: 10.1109/ISSCC.2019.8662432.
6. J. Schmenger, R. Kramer and M. März, "Active hybrid common mode filter for a highly integrated on-board charger for automotive applications," 2015 IEEE 13th Brazilian Power Electronics Conference and 1st Southern Power Electronics Conference (COBEP/SPEC), Fortaleza, 2015, pp. 1-7, doi: 10.1109/COBEP.2015.7420018.
7. K. Wu, Z. He, T. Yin and T. Zhang, "Digital Fast Charging System with Positive and Negative Pulse," 2017 IEEE 7th Annual International Conference on CYBER Technology in Automation, Control, and Intelligent Systems (CYBER), Honolulu, HI, 2017, pp. 1420-1424, doi: 10.1109/CYBER.2017.8446401.
8. B. Dragoi, "On selecting a front-end DC-DC converter for automotive applications," 2016 12th IEEE International Symposium on Electronics and Telecommunications (ISETC), Timisoara, 2016, pp. 29-32, doi: 10.1109/ISETC.2016.7781049.
9. J. Hu, Z. He, L. Lin, K. Xu and Y. Qiu, "Voltage Polarity Reversing-Based DC Short Circuit FRT Strategy for Symmetrical Bipolar FBSM-MMC HVDC System," in IEEE Journal of Emerging and Selected Topics in Power Electronics, vol. 6, no. 3, pp. 1008-1020, Sept. 2018, doi: 10.1109/JESTPE.2018.2820076.
10. A. Huang, Xin Yan, Jingdong Sun, Qiaolei Huang, Jun Fan, Songping Wu, Dave Zhang, Huan Liao, Shuai Jin and Zhiping Yang "Investigation and Mitigation of Radio Frequency Interference Caused by Weak Grounding of USB Type-C Receptacle Connector," 2020 IEEE International Symposium on Electromagnetic Compatibility & Signal/Power Integrity (EMCSI), Reno, NV, USA, 2020, pp. 139-144, doi: 10.1109/EMCSI38923.2020.9191587.
11. C. Rostamzadeh, F. Canavero and F. Kashefi, "Noise mitigation analysis of a  $\pi$ -filter for an automotive control module," 2010 IEEE International Symposium on Electromagnetic Compatibility, Fort Lauderdale, FL, 2010, pp. 591-596, doi: 10.1109/ISEMC.2010.5711343.

12. A. C. Chow and D. J. Perreault, "Active EMI filters for automotive motor drives," Power Electronics in Transportation, 2002, Auburn Hills, MI, USA, 2002, pp. 127-134, doi: 10.1109/PET.2002.1185560.
13. P. Giannelli, L. Capineri, G. Calabrese, G. Frattini and M. Granato, "A reduced output ripple step-up DC-DC converter for automotive LED lighting," 2017 13th Conference on Ph.D. Research in Microelectronics and Electronics (PRIME), Giardini Naxos, 2017, pp. 329-332, doi: 10.1109/PRIME.2017.7974174.
14. V. Patel and A. M., "Fault Management Strategy and PWM Monitoring for HVAC ECU," 2018 Second International Conference on Electronics, Communication and Aerospace Technology (ICECA), Coimbatore, 2018, pp. 1736-1739, doi: 10.1109/ICECA.2018.8474585.
15. Y. Wang, Z. Liu and J. Liu, "A Novel RC-Triggered Bidirectional ESD Protection Circuit in SOI Technology," 2019 8th International Symposium on Next Generation Electronics (ISNE), Zhengzhou, China, 2019, pp. 1-3, doi: 10.1109/ISNE.2019.8896534.
16. A. Kotlar and P. Svasta, "Protection supply circuit design for power electronics in automotive," 2017 40th International Spring Seminar on Electronics Technology (ISSE), Sofia, 2017, pp. 1-4, doi: 10.1109/ISSE.2017.8000975.

### AUTHORS PROFILE



**Ms. Raveena Jokim Crastha**, currently holding Master's degree in Digital Electronics and Communication specialization at Dayananda Sagar College of Engineering, Bengaluru and has received Bachelor's degree in Electronics and Communication specialization from Christ University Faculty of Engineering, Bengaluru. She has also worked as an intern in automotive design and manufacturing domain.

She has worked on several projects and has participated in international and national level journal conferences. She is currently working as a hardware design engineer in an automotive industry. Her areas of interests include Power system controls, Robotics, Digital electronics, and logic designs, Error control coding and Networking, Wireless communication, and embedded systems.



**Dr. Roopa M.**, has Completed Ph.D. degree in Applied Electronics Division with the Specialization of VLSI and Embedded Systems from Gulbarga University, Kalburgi. She is presently working as a professor in the department of Electronics and Communication at Dayananda Sagar College of Engineering, Bengaluru. She has presented papers at both National and International Conferences. She has

guided many UG and PG projects. She is also guiding PhD students and has a credit of one UG and 2PG degrees. She is having Professional Body membership in LMISTE, MIETE, MIEEE also, a member of BOS and BOE. She has Completed 30 years of Academic Service.